BIOCHEMISTRY
including biophysical chemistry & molecular biology
Article

Biochemistry **2010,** *49,* 5553–5559 5553
DOI: 10.1021/bi100542f

Allosteric Control of Promoter DNA Bending by Cyclic AMP Receptor and Cyclic AMP

Dietmar Porschke*

Max Planck Institut für biophysikalische Chemie, 37077 Göttingen, Germany

Received April 10, 2010; Revised Manuscript Received June 1, 2010

ABSTRACT: The structure of the cyclic AMP receptor−promoter complex in solution was studied in the range of 0.2−50 μM cAMP by measurements of the electric birefringence at 0.1 M salt using a lac promoter DNA with 121 bp and with the CAP binding site at its center. An excess of protein required for complete conversion of the promoter DNA into the specific complex seems to be partly due to nonspecific binding. The specific complex is associated with a decay time constant of 1.36 μs at 3 °C, a positive birefringence, and a permanent dipole moment demonstrated by pulse reversal. These attributes were observed at cAMP concentrations between 3 and 50 μM and are characteristic of the specific complex. Model calculations demonstrate that the DNA bending angle under these conditions is 92°. The observed positive birefringence does not result from the combination of the calculated quasi-permanent dipole and the orientation of the helix axes alone but is due to coupling of translational and rotational diffusion. When the cAMP concentration is decreased below 3 μM, the positive birefringence turns to a negative one with a transition center at 1.5 μM. The transition is too narrow for a model with induction of the specific cyclic AMP receptor−promoter complex after binding of a single cAMP to the cyclic AMP receptor dimer but is consistent with induction of this complex after binding of two cAMP molecules. The cyclic AMP receptor−promoter complex is driven into its specific bent form in vitro in the range of cAMP concentrations corresponding to that required for gene regulation in vivo.

The cyclic AMP receptor (CAP)[1] and its complex with promoter DNA constitute the paradigm for regulation of gene activity by protein-induced DNA bending (*1*) (cf. textbooks of biochemistry and molecular biology). An extensive literature exists with data on different properties of this protein, including binding parameters for cyclic AMP (*2*, *3*), specific and nonspecific DNA (*4*−*10*). The structure of the cAMP receptor protein was determined in its complex with cyclic AMP (*11*), in the complex with both cAMP and promoter DNA (*12*−*14*), and finally, the structure of the protein without ligands (*15*, *16*) was also determined. Contributions to allosteric control were analyzed by different approaches (*17*, *18*). Particular attention was devoted to protein-induced bending of promoter DNA. Investigations using X-ray crystallography (*12*, *14*), FRET (*19*−*21*), and cyclization (*22*) measurements provided bending angles in the range of 70−100°. These bending angles have been determined at relatively high concentrations of cAMP of 100 or 200 μM, which is far above the physiological range of cAMP concentrations demonstrated to be ∼1 μM (*23*, *24*). Initially, two cAMP binding sites were identified per protein dimer by X-ray crystallography (*11*). When the resolution was increased, another two binding sites for cAMP were detected (*13*). Titration experiments showed two concentration ranges of cAMP binding to the protein in the absence of DNA: a first one at ∼20 μM cAMP (*2*, *3*) and another at millimolar cAMP concentrations (*3*, *25*). Both of these concentration ranges are clearly above the cAMP levels used in gene regulation, "an enigma of the CAP system" discussed Lin and Lee (*10*). They presented evidence that the enigma can be resolved by "thermodynamic linkage" of cAMP and DNA binding (*10*). Another, similar set of binding parameters was given by Takahashi et al. (*4*). However, information about the structure of the protein−DNA complex and the DNA bending angle over a sufficiently wide range of cAMP concentrations, including physiological values, is not available.

Among the approaches used for the characterization of structures in solution, electro-optical methods (*26*, *27*) are known to be very sensitive, but in most cases their application was limited to low salt concentrations. A cable discharge technique (*27*, *28*) was used at high salt concentrations, but measurements were restricted to very short pulses of relatively high electric field strengths. These limitations are now eliminated by a new technique with a particularly high sensitivity. The technique can be applied at physiological levels of salt concentrations and at relatively low electric field strengths.

The prospects of this electro-optical project can be improved by a promoter DNA optimized for the given task: the DNA should be long enough for sufficiently large effects but not too long, to avoid complications resulting from flexibility. A 121 bp DNA fragment with the lac promoter site at the center and stable blunt ends was cloned for this investigation. The experimental data were compared with calculations on model constructs using the procedures of quantitative molecular electro-optics described previously (*27*). The results extend the information on the structure of the CAP−promoter complex over a wide range of cAMP concentrations. Direct observation of the transition of the promoter DNA from the standard state to the specific complex with CAP provides new details about the allosteric control of gene activation.

MATERIALS AND METHODS

DNA single strands with the plus and minus strand sequences of the primary CAP binding site (135 residues) were synthesized.

*To whom correspondence should be addressed. Phone: 0551-2011438. Fax: 0551-2011168. E-mail: dpoersc@gwdg.de.

[1]Abbreviations: CAP, cyclic AMP receptor; cAMP, cyclic AMP; buffer B, 90 mM NaCl, 20 mM Tris (pH 8.0), 2 mM DTT, and 0.1 mM EDTA.

Published on Web 06/14/2010

After the single strands had been annealed, the resulting double helix was cloned into the pUC19 vector. The plasmid DNA was grown and isolated by standard procedures. The designed DNA fragment was excised from the plasmid DNA by restriction endonuclease *Sma*I and after phenol extraction isolated by Sepharose column chromatography. The DNA fragment was purified further by preparative gel electrophoresis. The fragment proved to be homogeneous in polyacrylamide gels. The sequence of the fragment with 121 bp was determined by standard procedures (GGGCACGACA GGTTTCCCGA CTGGAAAGCG GGCAGTGAGC GCAACGCAAT TAATGTGAGT TAGCTCACTC ATTAGGCACC CCAGGCTTTA CACTTTATGC TTCCGGCTCC GTATGTTGCC C). The center of the CAP binding site is between base pairs 61 and 62. The sequence of this binding site is identical with that of the standard lac binding site (*29*). Throughout this work, the DNA fragment is denoted lac121. The single strands for the consensus DNA fragment with 40 bp were synthesized by adoption of the sequence described by Ebright et al. (*7*), but the single "dangling" G-residues at each end were omitted. The single strands were annealed in buffer B. The blunt-ended fragment with 80 bp was prepared as described in ref *30*. DNA concentrations were determined using an extinction coefficient per nucleotide of 6500 M^{-1} cm^{-1} at 260 nm. The cAMP receptor protein was prepared according to the procedure of Ghosaini et al. (*31*) and personal communications kindly provided by A. Kolb. CAP concentrations are always given in units of protein dimer and were determined using an extinction coefficient of 40800 M^{-1} cm^{-1} at 278 nm, used by most authors in the literature (*2*, *10*). Solutions were prepared for measurements in buffer B [90 mM NaCl, 20 mM Tris (pH 8.0), 2 mM DTT, and 0.1 mM EDTA]. Buffer, DNA, and cAMP were mixed together, before the CAP protein was added as the last component. The solutions with the final composition used for the measurements were then incubated at 37 °C for 20 min.

The birefringence data were measured by an instrument with the standard classical setup [cf. Fredericq and Houssier (*26*)] using components of particularly high quality. A solid state Nd:vanadate laser (Verdi, Coherent) was used as a light source. The light intensity (532 nm) used in the present measurements was 0.5 W cw. A novel construction of the cell body and of the cell windows was essential for allowing cell windows to reach a state of minimal strain (publication in preparation). The DC electric field pulses were generated by Cober model 606 pulse generators. The polarity was inverted automatically after each pulse application. The transients shown here represent averages of transients from 20 pulse applications. AC electric field pulses were generated by an arbitrary function generator (AFG 3101) from Tektronix together with a linear pulse power amplifier (LPPA 6020) from dressler HF-Technik GmbH (Stolberg, Germany). The optical path length of the cell was 20 mm; the electrode distance between the Pt electrodes was 2.68 mm. Time constants were evaluated by fitting of the transients as measured (light intensity as a function of time) via application of a deconvolution algorithm (*32*). The equations described by Fredericq and Houssier (*26*) were used for conversion of light intensities into optical retardation or birefringence.

The nucleic acid structures were generated by Namot version 2.1 (*33*). The electro-optical data were simulated from given model structures using the procedures of quantitative molecular electro-optics (*27*).

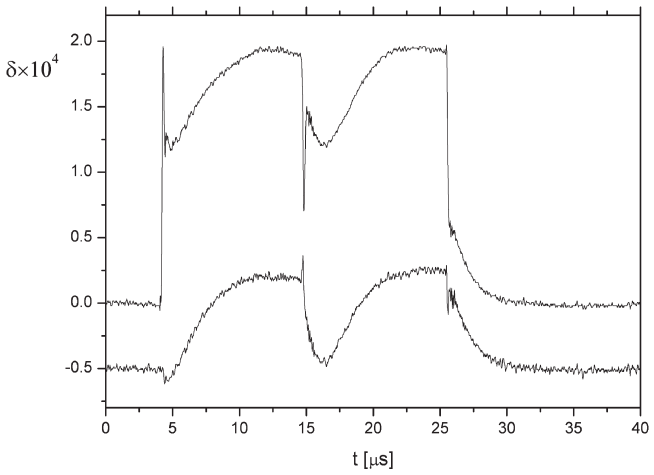

FIGURE 1: Optical retardation δ induced by an electric field pulse as a function of time t for the lac121−CAP complex in buffer B at 3 °C. The upper transient reflects the birefringence of the protein−nucleic acid complex together with that of the buffer, whereas the lower transient represents the birefringence of the protein−nucleic acid complex alone obtained by subtraction of the buffer signal measured separately. The lower transient is shifted by −0.5 units on the $\delta \times 10^4$-scale. The electric field of 1.65 kV/cm was applied at 4.04 μs; the field vector was reverted at 14.58 μs and finally was turned off at 25.5 μs. Concentrations: 0.156 μM DNA helix, 0.515 μM CAP, and 20 μM cAMP.

RESULTS

Birefringence Measurements. Because of the high sensitivity of the instrument, birefringence transients for the complex of CAP with the lac121 fragment (Figure 1) can be recorded at a satisfactory accuracy, even at a salt concentration of 100 mM used in this investigation. Part of the signal is given by the birefringence of water, which is clearly separated on the time scale from that of the protein DNA complex. The signal of the complex alone may be obtained by subtraction of the buffer signal measured under identical conditions (cf. Figure 1). All the transients for the CAP−lac121 complex measured at 100 mM salt show a positive birefringence, in contrast with the negative birefringence observed for the lac121−DNA alone under identical conditions. As shown by the signal induced upon pulse reversal, the protein−DNA complex reacts like molecules with a permanent dipole moment, again in contrast with the response of the DNA alone under identical conditions. The birefringence of the protein−DNA complex induced by high-frequency electric fields (1 MHz) is negligible, showing that any orientation due to an electric polarizability of the complex is small compared to that resulting from the permanent dipole.

The optical retardation obtained from the field-induced change of the light intensity increases with the square of the electric field strength (cf. Figure 2), and thus, the birefringence data are in the Kerr regime.

A parallel analysis of the protein−DNA complex by gel electrophoresis demonstrated the characteristic retardation of the electrophoretic mobility. Complete conversion of the band representing free DNA to the band representing the complex required an approximately 3-fold excess of the protein over the lac121−DNA fragment. The question of the stoichiometry was discussed by Garner et al. (*34*): they concluded that "only one of every four molecules in our preparation of CAP is active in specific binding". Similar comments on a reduced activity of the CAP protein in the range of 30−40% were included in several papers by other authors (*8*, *35*−*37*). The protein used in

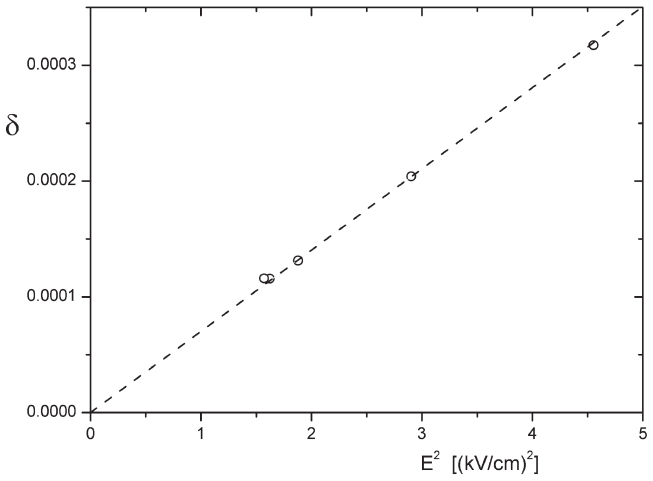

FIGURE 2: Optical retardation δ of a solution containing the lac121−CAP complex as a function of the square of the electric field strength (E^2) at 3 °C. Concentrations are the same as those listed in the legend of Figure 1.

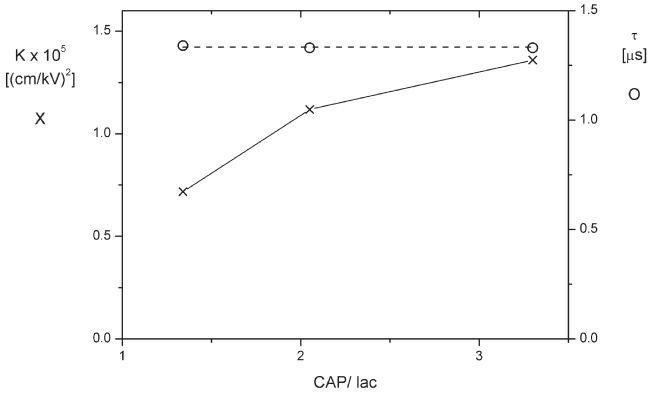

FIGURE 3: Kerr constant K (×, left scale) and birefringence decay time τ (○, right scale) for the lac121−CAP complex at different CAP/lac121 ratios at 3 °C in buffer B. Concentrations: 20 μM cAMP and 0.154 μM lac121.

the present experiments showed a single band in electrophoresis. Furthermore, the protein preparation was controlled by mass spectrometry and showed a single peak at the expected mass. For comparison, formation of the CAP−DNA complex was studied by gel electrophoresis using a synthetic DNA fragment with the consensus sequence (*7*) having 40 bp. In this case, the protein excess required for complete complex formation was reduced to a factor of ~1.4. This result suggests that the excess is required mainly because of nonspecific binding. More evidence for this conclusion is provided by birefringence experiments. Birefringence data obtained at different values of protein/DNA ratio r (cf. Figure 3) show an increase of the Kerr constant with an increase in r, whereas the decay time constant τ remains almost constant. Parallel birefringence experiments using a blunt-ended 84 bp DNA fragment without a specific CAP binding site (at the same concentration of protein and DNA phosphates in buffer B) showed an increase in the birefringence rise time of ~40%, whereas the decay time constant remained constant. This result indicates nonspecific binding because of a particularly high sensitivity of rise curves to binding of proteins. The high sensitivity results from the fact that (1) nonspecific binding at low degrees of saturation is nonsymmetric for the majority of binding states of a statistical distribution and (2) nonsymmetric

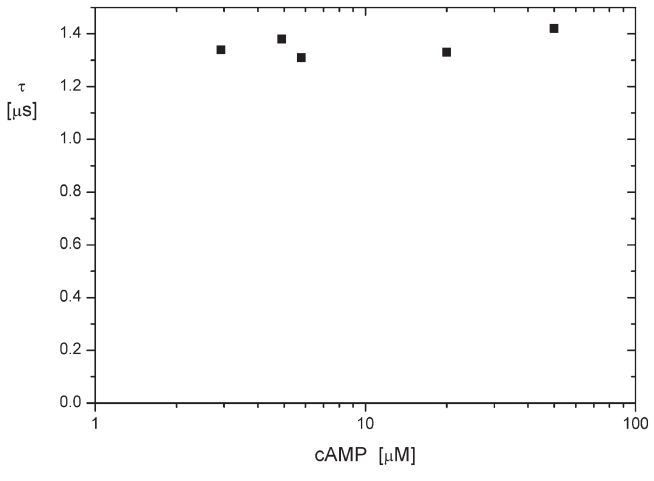

FIGURE 4: Birefringence decay time constant τ at different cAMP concentrations (at 3 °C in buffer B). The average of these τ values is 1.36 μs. Concentrations: 0.154 μM lac121 and 0.483 μM CAP.

binding is equivalent to a nonsymmetric charge distribution leading to a quasi-permanent dipole indicated by a particularly slow rise of the birefringence. This effect has been observed under various conditions (publication in preparation) and leads to a particularly high sensitivity of rise curves to protein binding, which is higher than that of decay curves. In this context, rise curves are used as a simple tool for qualitative detection of protein binding. Experimental data together with a more detailed discussion will be presented elsewhere.

Some problems associated with the excess of CAP for complete formation of the specific complex remain to be analyzed (cf. Discussion). The results described above indicate that complete formation of the specific complex under the given experimental conditions is associated with some nonspecific binding. However, the amount of nonspecific binding of CAP to the lac121 fragment under these conditions does not have any strong effect on the birefringence decay times. This is indicated by the fact that the birefringence decay time of the 84 bp fragment was not affected at the given protein per phosphate concentration. All experimental data described below were obtained for solutions having a 3-fold excess of CAP over the lac121 fragment. Birefringence decay times measured in the range of cAMP concentrations from 3 to 50 μM are constant within the limits of experimental accuracy (Figure 4). The average decay time constant derived from these measurements is 1.36 ± 0.06 μs.

Model Calculations. Models of the CAP−lac121 complex were constructed in two steps. First, the DNA was built using Namot (*33*) with a rise per base pair of 3.4 Å. Curvature was designed by setting selected values of tilt angles in the central block of 24 bp corresponding to the CAP binding domain. After completion of DNA construction and proper orientation of this construct, the protein extracted from Protein Data Bank (PDB) entry 1J59 (*14*) was simply added. An example of a resulting complex is shown in Figure 5. The final model does not represent the exact atomic details of DNA curvature observed in CAP−DNA crystals and also does not include the exact molecular contacts between the protein and the double helix, but this does not have any significant effect on the results of the simulation. The coordinates of complexes were read into the routines for automatic calculation of electro-optical parameters described previously (*27*). Simulation of electro-optical data requires the following steps: (1) conversion of the molecular structure to a bead model, which is used for calculation of the diffusion tensor,

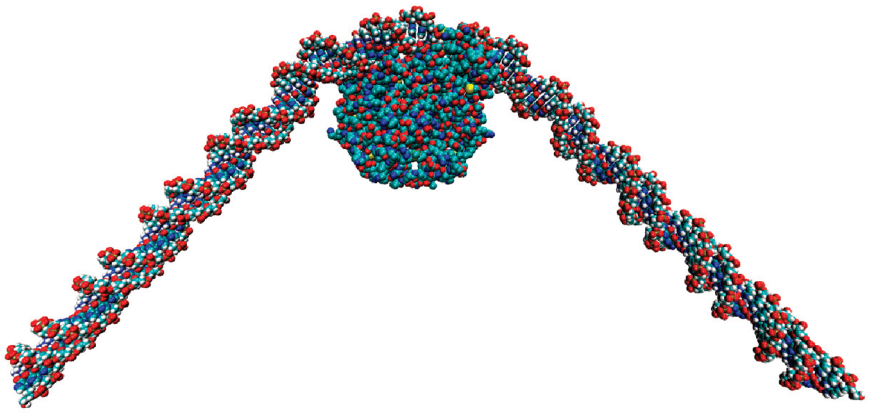

FIGURE 5: Model of the lac121−CAP complex with a DNA bending angle of 92°.

Table 1: Electro-Optical Parameters of the lac121−DNA and lac121−CAP Complexes at Different Bending Angles ϑ Obtained by Model Simulations[a]

	DNA alone						DNA with CAP					
					τ_2						τ_2	
ϑ	ξ_∞	μ (D)	decay	τ_1 at 20 °C	20 °C	3 °C	ξ_∞	μ (D)	decay	τ_1 at 20 °C	20 °C	3 °C
0	−1.486	82	mono		1185	2031	0.715	1228	mono		1378	2363
45	0.430	736	bi_max	117	1049	1798	0.429	1255	bi_max	181	1140	1954
71.5	0.065	1274	bi_max	194	873	1496	0.044	1431	bi_max	246	949	1627
85.2	−0.150	1528	bi_min	233	774	1327	−0.163	1524	bi_min	284	846	1451
94	−0.297	1674	bi_min	258	707	1212	−0.300	1584	bi_min	311	781	1338
98	−0.370	1737	bi_min	269	674	1155	−0.372	1604	bi_min	322	746	1278
107	−0.514	1838	bi_mm	289	608	1042	−0.490	1821	bi_mm	338	674	1155
125	−0.778	1930	bi	313	482	827	−0.760	1584	bi	362	529	907
142	−0.993	1859	bi	305	386	662	−0.965	1426	bi	347	442	758
177	−1.207	1148	mono		316	541	−1.022	720	mono		385	660

[a] ξ_∞ is the limit value of the reduced electric dichroism. μ is the quasi-permanent dipole moment. Decay describes the shape of the decay curves: mono, monoexponential; bi_max, biexponential with a maximum; bi_min, biexponential with a minimum; bi_mm, biexponential with a hardly visible minimum; bi, biexponential without inversion. Time constants (τ) are given in nanoseconds at 20 and 3 °C, as indicated. The values are given in full numerical detail, which may be useful for seeing trends in some cases. The accuracy is estimated to be ±1%.

(2) construction of an overall extinction tensor from the optical parameters for the residues contributing to absorbance, and (3) calculation of the dipole vector from the coordinates of charged residues. DNA phosphate charges were assumed to be 12% of the elementary charge. According to the polyelectrolyte theory of Manning (*38*), the phosphate charge remaining after ion condensation in the presence of monovalent ions is 24% of the elementary charge, but a major part of this charge is shielded by the ion atmosphere. The charge value appropriate for electro-optical calculations under the present experimental conditions remains to be established. It should be noted that the value used for the phosphate charge affects the magnitude of calculated dipole moments but does not affect the decay time constants. Thus, the evaluation of bending angles is also not affected. The charges of amino acid residues were calculated corresponding to standard p*K* values (see ref *27*). The diffusion tensor, the extinction tensor, and the dipole vector are used for calculation of electro-optical transients with the equations of Wegener et al. (*39*). The electro-optical data are calculated in the form of the electric dichroism. Because electro-optical effects of nucleic acids mainly result from the optical anisotropy of the base pairs, the electric dichroism and the electric birefringence are closely related and the sign of these parameters is equivalent. Thus, positive values of the electric dichroism correspond to positive values of the electric birefringence.

Electro-optical parameters were calculated for models with different bending angles (cf. Table 1). A graphical representation of the decay time constants τ_2 as a function of bending angle φ (cf. Figure 6) demonstrates the strong dependence of τ_2 on φ. A linear fit of the central part of this dependence and a comparison with the experimental τ_2 demonstrate a bending angle φ of 92° for the complex of CAP with the lac promoter DNA at 100 mM salt.

The stationary dichroism predicted by the calculations for complexes with bending angles (φ) around 92° is negative, whereas the observed stationary electric birefringence is positive. Simulations by Brownian dynamics demonstrate that translational−rotational coupling (*40*−*42*) induces a shift of the stationary dichroism or birefringence to positive values at low electric field strengths corresponding to those used in the experiments. These effects resulting from translational−rotational coupling have been described in detail for smoothly bent DNA (*43*, *44*) and are expected for large, nonsymmetric objects with a high net charge. In addition to this large effect on the stationary values, another relatively small effect should be mentioned. Because Namot does not provide a convenient way to introduce propeller twist, the DNA models were constructed with most of the base pairs perpendicular to the helix axis. Consideration of the propeller twist would reduce the absolute ξ_∞ values given in Table 1 by approximately 20%. The other parameters would not be affected within the limits of accuracy estimated to be ±1%.

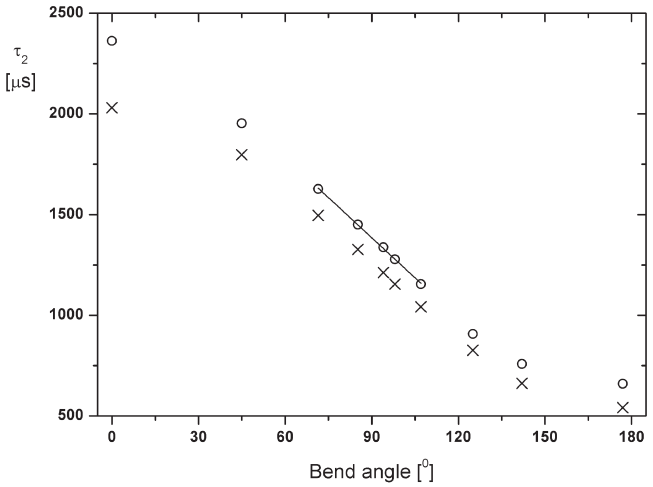

FIGURE 6: Decay time constant τ_2 calculated as a function of the bending angle for the lac121−DNA without protein (×) and for the lac121−CAP complex (○) at 3 °C. The straight line obtained by linear regression of the data between 71.5 and 107° (ϑ) was used for the evaluation of the bending angle.

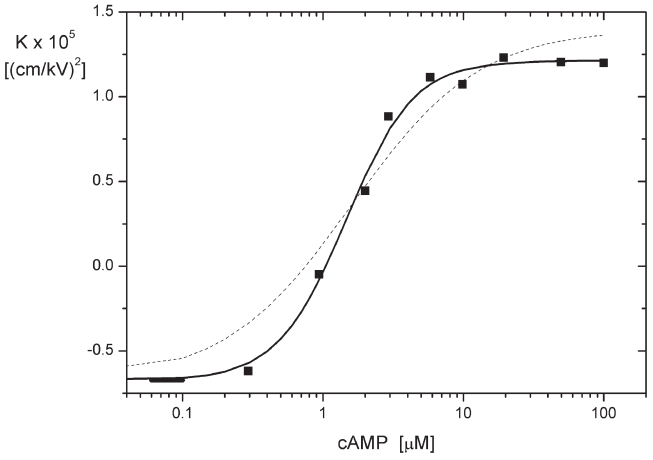

FIGURE 7: Kerr constant K as a function of the cAMP concentration (3 °C, buffer B, 0.154 μM lac121, 0.487 μM CAP). The solid line represents a fit by the model with two cAMP molecules per CAP dimer required for specific binding (for the parameters, see the text). The dashed line represent a least-squares fit by the model with one cAMP molecule per CAP dimer required for specific binding. The bar represents the Kerr constant of lac121-DNA in the absence of protein.

Transition of the Structure at Low cAMP Concentrations. The data described above were obtained at cAMP concentrations clearly greater than those used in vivo for the regulation of transcription. The state of the CAP−promoter system in the critical concentration range can be recorded by measurements of the Kerr constant. As shown in Figure 7, the Kerr constant is positive in the range of high cAMP concentrations but decreases to negative values when the cAMP concentration is below 1 μM. These data describe the transition of the promoter DNA from the bent state in its complex with CAP at high cAMP concentrations (> 3 μM) to the standard straight state at low cAMP concentrations (≤0.1 μM). At low cAMP concentrations, the affinity of CAP for DNA is reduced such that binding both to nonspecific DNA and to lac-promoter DNA is negligible under the conditions of the experiments described here (*4*−*10*).

A first attempt to describe the transition between these two limit states is based on a scheme with two reaction steps: (1) binding of a single cAMP to the protein dimer and (2) binding of this cAMP−protein complex to the specific DNA site. This model is not sufficient to describe the experimental data (dashed line in Figure 7), because the transition predicted by this model is much broader than that observed.

A second model includes two steps of cAMP binding to the protein and implies that the protein dimer with two cAMP binds to the specific DNA site:

$$\mathrm{CAP} + \mathrm{cAMP} \overset{K_1}{\rightleftarrows} \mathrm{CAP-cAMP}$$

$$\mathrm{CAP-cAMP} + \mathrm{cAMP} \overset{K_2}{\rightleftarrows} \mathrm{CAP-(cAMP)_2}$$

$$\mathrm{CAP-(cAMP)_2} + \mathrm{lac121} \overset{K_3}{\rightleftarrows} \mathrm{CAP-(cAMP)_2-lac121}$$

This model describes the experimental data very well (solid line in Figure 7). Least-squares fits show that a wide range of different parameter combinations is consistent with the data in Figure 7. When a low K_1 value is used, this can be compensated by an increase in K_2. When K_1 is fixed at 6.4×10^4 M^{-1}, a value obtained by Lin and Lee (*3*) in a recent analysis for the first step of cAMP binding to CAP, the other parameters were fitted to a K_2 of 3.1×10^4 M^{-1} and a K_3 of 8.2×10^8 M^{-1}. The K_1 and K_2 values are macroscopic as defined by the equations given above; the microscopic values K_1^m and K_2^m, considering that the first cAMP has access to two sites and dissociation of cAMP from the CAP−$(cAMP)_2$ complex occurs from two sites, are given by the relations $K_1 = 2K_1^m$ and $K_2 = {}^1/_2K_2^m$, respectively. The K_2 value obtained from fitting of the data in Figure 7 is very close to that derived independently by Lin and Lee (*3*) from fluorescence and calorimetric measurements. Finally, the value of K_3 is also in the range expected from literature data (*4*, *10*).

DISCUSSION

The main goal of this investigation was an analysis of the formation of the CAP−promoter complex close to physiological conditions. The electro-optical procedure used for analysis has been developed in recent years to a state with a significantly increased sensitivity, such that measurements at physiological salt are possible at low concentrations of macromolecules at a remarkably high accuracy.

Nonspecific Complexes and the Stoichiometry Problem. An example of the high sensitivity is provided by the detection of nonspecific binding under conditions with very low degrees of binding. This is due to the fact that binding of a single protein molecule or a few protein molecules to a DNA fragment is nonsymmetric with a high probability. The loss of symmetry induces a change in the orientation mechanism and a large change in the rise time. Under the same conditions, the decay curves remain almost unaffected. In this investigation, rise curves have been used only for the qualitative detection of nonspecific binding and were not used for an analysis of specific complexes. The electro-optical results together with the dependence of the stoichiometry on the DNA chain length provide evidence that the excess of CAP required for complete formation of the specific complex is not due to the partial inactivity of CAP samples but to nonspecific binding.

The equilibrium constants reported in the literature (*4*−*10*) for the binding of CAP to specific and nonspecific DNA indicate that specific sites should be saturated almost completely before

nonspecific sites are occupied. According to these equilibrium parameters, nonspecific binding is hardly expected to be the basis of the stoichiometry problem. Because of the large excess of nonspecific sites, these sites will be occupied preferentially in the first phase of the binding reaction. Measurements of the binding kinetics demonstrate that the transfer from nonspecific to specific complexes is relatively slow in the case of CAP (publication in preparation). However, all samples used in this investigation were equilibrated for a relatively long period of time (cf. Materials and Methods). If the incubation times were sufficient for complete equilibration, another closely related interpretation has to be considered: the stoichiometry problem may be due to the existence of pseudobinding sites. Pseudosites with sequences similar to that of the specific site are expected to appear at a relatively high probability (*45*). Few pseudosites with an affinity intermediate between that of specific and nonspecific sites would be sufficient to resolve the stoichiometry problem. Further investigations are required for a final explanation. In addition to these effects, some contribution to the stoichiometry problem may result from the tendency of CAP to stick to surfaces. Sticking of CAP to surfaces was observed to cause serious perturbations of fluorescence titrations at ≤ 0.1 μM CAP.

Specific Complex. The experimental decay time constants obtained for the specific complex are compared with data simulated for molecular models based on the algorithms (*27*) of "quantitative molecular electro-optics". The bending angle of 92° derived from these electro-optical measurements is close to the value of 85−90° obtained by Kahn and Crothers (*22*) from cyclization data at 100 μM cAMP and also to the values of 90° and 87° observed in crystal structures grown at 2 mM cAMP by Schultz, Shields, and Steitz (*12*) and Parkinson et al. (*14*), respectively. Compared to these results, the bending angle of $77 \pm 3°$ determined by FRET measurements (*19*) at 200 μM cAMP is relatively low. Electro-optical measurements at salt concentrations below 100 mM indicate that more compact structures with more extensive DNA bending are formed at low salt concentrations (publication in preparation).

Regulation of Gene Activity. The allosteric control of CAP binding and DNA bending under physiological conditions seemed to be a problem, because the concentration of cAMP required for binding to the protein in vitro and the cAMP level used for gene regulation in vivo are different by a factor of ~100. As discussed by Lin and Lee (*10*), the "enigma" can be resolved by thermodynamic linkage: cAMP−CAP complexes have a higher affinity for promoter DNA, implying a higher affinity of cAMP for the CAP−promoter complex than for CAP alone (cf. also ref *4*). However, the overall affinity of the CAP protein for the promoter DNA may not be a sufficient criterion, because the biological activity is expected to be dependent on the formation of the specific bent complex. Another question remained with respect to the stoichiometry of cAMP activation. Several papers (*4*, *10*, *25*) have claimed that binding of a single cAMP molecule per CAP dimer is sufficient for activation. The recently determined structure of the apoprotein (*15*, *16*) demonstrates that large changes in the conformation must be induced by cAMP to release the DNA binding domain from an embedded state. Release of both domains in the CAP dimer and, thus, cAMP binding to both subunits appears to be required for specific binding to the promoter. The experimental data presented in Figure 7 provide clear evidence that two cAMP molecules per protein dimer are required for activation. The Kerr constant is a quantity representing the transition from the bend complex to the free DNA selectively. This is due to the fact that the bend complex is associated with a permanent dipole and a positive birefringence, whereas the free DNA has an induced dipole and a negative birefringence. Other protein−DNA complexes without DNA bending, which may exist in a distribution of states in solution, are not reflected in this signal, at least not explicitly. The data are described by the three-step model in a convincing manner, first because the fit represents the experimental points within the limits of experimental accuracy and second because the resulting binding constants are consistent with corresponding parameters determined independently by completely different methods (*4*, *10*). Finally, the midpoint of the relatively narrow transition, determined in vitro under conditions close to those in vivo, appears at a cAMP concentration level very close to that found for regulation of gene activity in vivo (*23*, *24*). An exact specification of in vivo conditions with respect to the free CAP concentration is hardly possible. The total concentration of CAP in bacterial cells (*46*) is ~2.5 μM, but a major part is expected to be bound to nonspecific DNA, because the total concentration of nonspecific DNA sites is ~10 mM. The amount of CAP bound to nonspecific DNA cannot be specified exactly, partly because the degree of binding to DNA by various proteins and other ligands is not known sufficiently well. In most of the present experiments, the total CAP concentration was ~0.5 μM, the total concentration of specific sites was ~0.15 μM, and the concentration of nonspecific sites was ~20 μM. In an *Escherichia coli* cell, one lac promoter corresponds to a concentration of ~2 nM, but there are more than 20 operons activated by CAP, resulting in a concentration of specific sites of ~0.04 μM, rather close to that used in the present experiments. A major difference between the in vitro and in vivo conditions is the huge excess of nonspecific sites in vivo, which is an essential factor in the kinetics (publication in preparation).

ACKNOWLEDGMENT

The facilities of the Gesellschaft für wissenschaftliche Datenverarbeitung mbH (Göttingen, Germany) were used for the evaluation and simulations of data. The linear pulse power amplifier (LPPA 6020) was generously provided by GSI Helmholtzzentrum für Schwerionenforschung GmbH (Darmstadt, Germany). The advice of Dr. Manfred Konrad during cloning and the technical assistance of Jürgen Wawrzinek in DNA preparation are gratefully acknowledged.

REFERENCES

1. Kolb, A., Busby, S., Buc, H., Garges, S., and Adhya, S. (1993) Transcriptional Regulation by cAMP and Its Receptor Protein. *Annu. Rev. Biochem. 62*, 749–795.
2. Takahashi, M., Blazy, B., and Baudras, A. (1980) An Equilibrium Study of the Cooperative Binding of Adenosine Cyclic 3′,5′-Monophosphate and Guanosine Cyclic 3′,5′-Monophosphate to the Adenosine Cyclic 3′,5′-Monophosphate Receptor Protein from *Escherichia coli*. *Biochemistry 19*, 5124–5130.
3. Lin, S. H., and Lee, J. C. (2002) Communications between the high-affinity cyclic nucleotide binding sites in *E. coli* cyclic AMP receptor protein: Effect of single site mutations. *Biochemistry 41*, 11857–11867.
4. Takahashi, M., Blazy, B., Baudras, A., and Hillen, W. (1989) Ligand-Modulated Binding of a Gene Regulatory Protein to DNA: Quantitative Analysis of Cyclic Amp Induced Binding of CRP from *Escherichia coli* to Non-Specific and Specific DNA Targets. *J. Mol. Biol. 207*, 783–796.
5. Saxe, S. A., and Revzin, A. (1979) Cooperative Binding to DNA of Catabolite Activator Protein of *Escherichia coli*. *Biochemistry 18*, 255–263.

6. Giraudpanis, M. J., Toulme, F., Blazy, B., Maurizot, J. C., and Culard, F. (1994) Fluorescence Study on the Nonspecific Binding of Cyclic-AMP Receptor Protein to DNA: Effect of pH. *Biochimie 76*, 133–139.
7. Ebright, R. H., Ebright, Y. W., and Gunasekera, A. (1989) Consensus DNA Site for the *Escherichia coli* Catabolite Gene Activator Protein (CAP): CAP Exhibits a 450-Fold Higher Affinity for the Consensus DNA Site Than for the *Escherichia coli* Lac DNA Site. *Nucleic Acids Res. 17*, 10295–10305.
8. Fried, M. G., and Crothers, D. M. (1984) Equilibrium Studies of the Cyclic-Amp Receptor Protein-DNA Interaction. *J. Mol. Biol. 172*, 241–262.
9. Liu-Johnson, H. N., Gartenberg, M. R., and Crothers, D. M. (1986) The DNA-Binding Domain and Bending Angle of *Escherichia coli* CAP Protein. *Cell 47*, 995–1005.
10. Lin, S. H., and Lee, J. C. (2002) Linkage of multiequilibria in DNA recognition by the D53H *Escherichia coli*, cAMP receptor protein. *Biochemistry 41*, 14935–14943.
11. McKay, D. B., and Steitz, T. A. (1981) Structure of Catabolite Gene Activator Protein at 2.9 Å Resolution Suggests Binding to Left-Handed B-DNA. *Nature 290*, 744–749.
12. Schultz, S. C., Shields, G. C., and Steitz, T. A. (1991) Crystal Structure of a CAP-DNA Complex: The DNA Is Bent by 90°. *Science 253*, 1001–1007.
13. Passner, J. M., and Steitz, T. A. (1997) The structure of a CAP-DNA complex having two cAMP molecules bound to each monomer. *Proc. Natl. Acad. Sci. U.S.A. 94*, 2843–2847.
14. Parkinson, G., Wilson, C., Gunasekera, A., Ebright, Y. W., Ebright, R. E., and Berman, H. M. (1996) Structure of the CAP-DNA complex at 2.5 angstrom resolution: A complete picture of the protein-DNA interface. *J. Mol. Biol. 260*, 395–408.
15. Popovych, N., Tzeng, S. R., Tonelli, M., Ebright, R. H., and Kalodimos, C. G. (2009) Structural basis for cAMP-mediated allosteric control of the catabolite activator protein. *Proc. Natl. Acad. Sci. U.S.A. 106*, 6927–6932.
16. Sharma, H., Yu, S. N., Kong, J. L., Wang, J. M., and Steitz, T. A. (2009) Structure of apo-CAP reveals that large conformational changes are necessary for DNA binding. *Proc. Natl. Acad. Sci. U.S. A. 106*, 16604–16609.
17. Fic, E., Bonarek, P., Gorecki, A., Kedracka-Krok, S., Mikolajczak, J., Polit, A., Tworzydlo, M., Dziedzicka-Wasylewska, M., and Wasylewski, Z. (2009) cAMP Receptor Protein from *Escherichia coli* as a Model of Signal Transduction in Proteins: A Review. *J. Mol. Microbiol. Biotechnol. 17*, 1–11.
18. Tzeng, S. R., and Kalodimos, C. G. (2009) Dynamic activation of an allosteric regulatory protein. *Nature 462*, 368–372.
19. Kapanidis, A. N., Ebright, Y. W., Ludescher, R. D., Chan, S., and Ebright, R. H. (2001) Mean DNA bend angle and distribution of DNA bend angles in the CAP-DNA complex in solution. *J. Mol. Biol. 312*, 453–468.
20. Heyduk, T., and Lee, J. C. (1992) Solution Studies on the Structure of Bent DNA in the cAMP Receptor Protein-Lac DNA Complex. *Biochemistry 31*, 5165–5171.
21. Lin, S. H., and Lee, J. C. (2003) Determinants of DNA bending in the DNA-cyclic AMP receptor protein complexes in *Escherichia coli*. *Biochemistry 42*, 4809–4818.
22. Kahn, J. D., and Crothers, D. M. (1998) Measurement of the DNA bend angle induced by the catabolite activator protein using Monte Carlo simulation of cyclization kinetics. *J. Mol. Biol. 276*, 287–309.
23. Lis, J. T., and Schleif, R. (1973) Different Cyclic-AMP Requirements for Induction of Arabinose and Lactose Operons of *Escherichia coli*. *J. Mol. Biol. 79*, 149–162.
24. Epstein, W., Rothmandenes, L. B., and Hesse, J. (1975) Adenosine 3′,5′-Cyclic Monophosphate as Mediator of Catabolite Repression in *Escherichia coli*. *Proc. Natl. Acad. Sci. U.S.A. 72*, 2300–2304.
25. Heyduk, T., and Lee, J. C. (1989) *Escherichia coli* cAMP Receptor Protein: Evidence for 3 Protein Conformational States with Different Promoter Binding Affinities. *Biochemistry 28*, 6914–6924.
26. Fredericq, E., and Houssier, C. (1973) Electric dichroism and electric birefringence, Clarendon Press, Oxford, U.K.
27. Porschke, D., and Antosiewicz, J. M. (2007) Quantitative molecular electro-optics: Macromolecular structures and their dynamics in solution. In Molecular and colloidal electro-optics (Stoylov, S. P., and Stoimenova, M. V., Eds.) pp 55−1007, CRC, Boca Raton, FL.
28. MeyerAlmes, F. J., and Porschke, D. (1997) The cyclic AMP receptor promoter DNA complex: A comparison of crystal and solution structure by quantitative molecular electrooptics. *J. Mol. Biol. 269*, 842–850.
29. Reznikoff, W. S., and Abelson, J. N. (1978) The lac Promoter. In The Operon (Miller, J. H., and Reznikoff, W. S., Eds.) Cold Spring Harbor Laboratory Press, Plainview, NY.
30. Porschke, D. (1991) Persistence Length and Bending Dynamics of DNA from Electrooptical Measurements at High Salt Concentrations. *Biophys. Chem. 40*, 169–179.
31. Ghosaini, L. R., Brown, A. M., and Sturtevant, J. M. (1988) Scanning Calorimetric Study of the Thermal Unfolding of Catabolite Activator Protein from *Escherichia coli* in the Absence and Presence of Cyclic Mononucleotides. *Biochemistry 27*, 5257–5261.
32. Porschke, D., and Jung, M. (1985) The Conformation of Single Stranded Oligonucleotides and of Oligonucleotide-Oligopeptide Complexes from Their Rotation Relaxation in the Nanosecond Time Range. *J. Biomol. Struct. Dyn. 2*, 1173–1184.
33. Tung, C. S., and Carter, E. S. (1994) Nucleic-Acid Modeling Tool (Namot): An Interactive Graphic Tool for Modeling Nucleic-Acid Structures. *Comput. Appl. Biosci. 10*, 427–433.
34. Garner, M. M., and Revzin, A. (1982) Stoichiometry of Catabolite Activator Protein Adenosine Cyclic 3′,5′-Monophosphate Interactions at the Lac Promoter of *Escherichia coli*. *Biochemistry 21*, 6032–6036.
35. Fried, M. G., and Crothers, D. M. (1984) Kinetics and Mechanism in the Reaction of Gene Regulatory Proteins with DNA. *J. Mol. Biol. 172*, 263–282.
36. Zinkel, S. S., and Crothers, D. M. (1990) Comparative Gel Electrophoresis Measurement of the DNA Bend Angle Induced by the Catabolite Activator Protein. *Biopolymers 29*, 29–38.
37. Menendez, M., Kolb, A., and Buc, H. (1987) A New Target for CRP Action at the malT Promoter. *EMBO J. 6*, 4227–4234.
38. Manning, G. S. (1978) Molecular Theory of Polyelectrolyte Solutions with Applications to Electrostatic Properties of Polynucleotides. *Q. Rev. Biophys. 11*, 179–246.
39. Wegener, W. A., Dowben, R. M., and Koester, V. J. (1979) Time-Dependent Birefringence, Linear Dichroism, and Optical Rotation Resulting from Rigid-Body Rotational Diffusion. *J. Chem. Phys. 70*, 622–632.
40. Brenner, H. (1965) Coupling between the Translational and Rotational Brownian Motions of Rigid Particles of Arbitrary Shape. I. Helicoidally Isotropic Particles. *J. Colloid Sci. 20*, 104–122.
41. Brenner, H. (1967) Coupling between Translational and Rotational Brownian Motions of Rigid Particles of Arbitrary Shape. 2. General Theory. *J. Colloid Interface Sci. 23*, 407–436.
42. Wegener, W. A. (1986) Transient Electric Birefringence of Dilute Rigid-Body Suspensions at Low Field Strengths. *J. Chem. Phys. 84*, 5989–6004.
43. Porschke, D., and Antosiewicz, J. M. (2005) Strong effect of hydrodynamic coupling on the electric dichroism of bent rods. *J. Phys. Chem. B 109*, 1034–1038.
44. Antosiewicz, J. M., and Porschke, D. (2009) Effects of Hydrodynamic Coupling on Electro-Optical Transients. *J. Phys. Chem. B 113*, 13988–13992.
45. Berg, O. G., and von Hippel, P. H. (1988) Selection of DNA-Binding Sites by Regulatory Proteins. 2. The Binding Specificity of Cyclic-AMP Receptor Protein to Recognition Sites. *J. Mol. Biol. 200*, 709–723.
46. Zubay, G. (1980) The Isolation and Properties of CAP, the Catabolite Gene Activator. *Methods Enzymol. 65*, 856–877.